

See discussions, stats, and author profiles for this publication at: <https://www.researchgate.net/publication/221876586>

Persistent Source Influences on the Trailing Edge of a Groundwater Plume, and Natural Attenuation Timeframes: The F-Area Savannah River Site

ARTICLE in ENVIRONMENTAL SCIENCE & TECHNOLOGY · MARCH 2012

Impact Factor: 5.33 · DOI: 10.1021/es204265q · Source: PubMed

CITATIONS

6

READS

171

5 AUTHORS, INCLUDING:



Jiamin Wan

Lawrence Berkeley National Laboratory

126 PUBLICATIONS 2,658 CITATIONS

[SEE PROFILE](#)



Tetsu K. Tokunaga

Lawrence Berkeley National Laboratory

156 PUBLICATIONS 2,937 CITATIONS

[SEE PROFILE](#)



Wenming Dong

Lawrence Berkeley National Laboratory

63 PUBLICATIONS 996 CITATIONS

[SEE PROFILE](#)



Susan Sharpess Hubbard

Lawrence Berkeley National Laboratory

248 PUBLICATIONS 3,392 CITATIONS

[SEE PROFILE](#)

Persistent Source Influences on the Trailing Edge of a Groundwater Plume, and Natural Attenuation Timeframes: The F-Area Savannah River Site

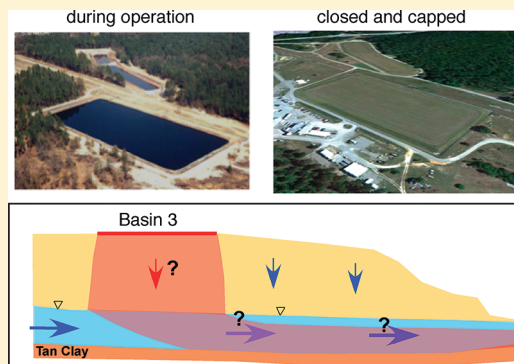
Jiamin Wan,^{†,*} Tetsu K. Tokunaga,[†] Wenming Dong,[†] Miles E. Denham,[‡] and Susan S. Hubbard[†]

[†]Earth Sciences Division, Lawrence Berkeley National Laboratory (LBNL), Berkeley, California

[‡]Savannah River National Laboratory (SRNL), Aiken, South Carolina

Supporting Information

ABSTRACT: At the Savannah River Site's F-Area, wastewaters containing radionuclides were disposed into seepage basins for decades. After closure and capping in 1991, the U.S. Department of Energy (DOE) has been monitoring and remediating the groundwater plume. Despite numerous studies of the plume, its persistence for over 20 years has not been well understood. To better understand the plume dynamics, a limited number of deep boreholes were drilled to determine the current plume characteristics. A mixing model was developed to predict plume tritium and nitrate concentrations. We found that the plume trailing edges have emerged for some contaminants, and that contaminant recharge from the basin's vadose zone is still important. The model's estimated time-dependent basin drainage rates combined with dilution from natural recharge successfully predicted plume tritium and nitrate concentrations. This new understanding of source zone influences can help guide science-based remediation, and improve predictions of the natural attenuation timeframes.



INTRODUCTION

Past disposal of large volumes of wastewaters at mining, weapons production, and industrial sites have left groundwater at many locations contaminated, even decades after cessation of operations. In such environments, determining plume dynamics is essential for predicting remediation and natural attenuation timeframes. The Savannah River Site (SRS, South Carolina) was a nuclear processing facility operated during the Cold War, where voluminous quantities of wastewaters were disposed into aquifers via seepage basins. The SRS F-Area seepage basins were used to dispose of approximately $7 \times 10^6 \text{ m}^3$ of acidic waste solutions containing multiple radionuclides, metals, and nitrate from 1955 to 1988.¹ The waste solutions contained more than a dozen different radioactive elements including $^{235\&238}\text{U}$, $^{238\&239}\text{Pu}$, ^3H , ^{90}Sr , ^{129}I , ^{241}Am , $^{141\&144}\text{Ce}$, and $^{137\&139}\text{Cs}$, and nonradioactive contaminants such as Hg, Pb, Cd, Cr, and As. Large quantities of HNO_3 and NaOH were also discharged into the basins. The average pH of the influent waste solutions was 2.9, but values ranged from pH 1.5 to 13. The DOE has been monitoring the groundwater in the F-Area through an array of wells since 1951, and contaminants were detected in groundwater and Fourmile Branch (Figure 1) as early as 1979.²

Discharges to the basins were terminated in November 1988, their most contaminated soils were removed, and their surfaces were capped in 1991.³ It is worth noting that waste disposal into seepage basins was common practice at weapons facilities

during the Cold War, and resulted in similar groundwater plumes at other locations such as the S-3 Ponds in Oak Ridge Reservation (Tennessee) and the 300 Area in the Hanford Site (Washington). These seepage basins have all been dewatered, partially excavated, capped, and subjected to costly groundwater remediation and monitoring. Given the persistence of these contaminant plumes, DOE is currently searching for sustainable remediation strategies, including monitored natural attenuation.

Basin-3 was the largest and the most permeable F-Area seepage basin (2.0 ha), with the water table at about 20 m depth. The groundwater flow direction (Figure 1) is toward Fourmile Branch, with an average water table gradient of approximately 0.014 between Basin-3 and Fourmile Branch, and 0.007 near the basin.⁴ The groundwater velocity averages about 124 m yr^{-1} in the 10 m thick, unconfined Upper Aquifer, underlain by the Tan Clay confining bed (average 2.5 m thick) that partly inhibited downward migration of the contaminants. This study focuses on the contaminated Upper Aquifer only, which consists of Tertiary age barrier beach and Lagoonal deposits.⁵ Mechanisms responsible for F-Area contaminant migration have been evaluated in many studies.^{6–11} Serkiz et al.¹² used sequential extraction of contaminated F-Area

Received: November 28, 2011

Revised: March 18, 2012

Accepted: March 20, 2012

Published: March 20, 2012

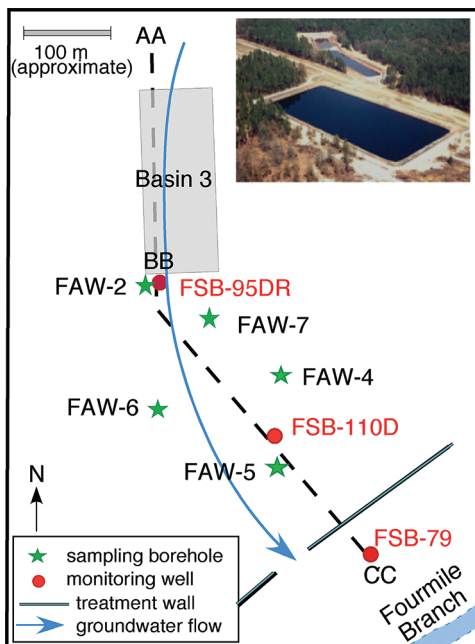


Figure 1. Basin 3 area map showing the spatial relations among the five sampling boreholes, three historical monitoring wells, groundwater flow direction, and Fourmile Branch. The insert is a historical photograph of the seepage basins for waste solution disposal during the years of 1955–1988.

sediments to evaluate U partitioning. Dong et al.¹³ determined that kaolinite is a more important sorbent for U(VI) at pH < 4.0, while goethite plays major role at pH > 4.0. The rising ¹²⁹I concentrations in recent years is attributed to its increased mobility in response to gradual increases in pH, as discussed in recent studies.^{5,14,15} Drainage rates beneath the basin have been estimated at about 0.5 m y⁻¹ during initial dewatering, declining to several cm y⁻¹ after 20 years.¹⁶ The groundwater monitoring data show that currently the plume remains acidic, and concentrations of U, ⁹⁰Sr, ¹²⁹I, ³H, and NO₃⁻ are still many times higher than their maximum contaminant levels (MCLs).

At the SRS F-Area, several remedial actions have been performed since basin closure. Pump-treat-reinjection remediation was conducted in the vicinity of Basin-3, from 1997 to 2003. The goal of the treatment system was to remove metals and radionuclides using reverse osmosis, precipitation/flocculation, and ion exchange. The plume water was pumped out at various locations downstream and the treated water was reinjected from upstream of the basin. Tritium and nitrate were not the targets of the treatments, so their concentrations do not appear affected (groundwater monitoring data presented later). Barrier wall emplacement and pH neutralization treatment was initiated in 2004 (locations of the installed barrier and treatment walls are shown in Figure 1), with alkaline solutions injected periodically to neutralize the acidic groundwater.³ The walls, set into the Tan Clay, were made of cement-like material for directing the water flow to the gate where the base was added.

The objective of this work was to develop a method to address the issues of source zone related plume development through time and space in the subsurface. Within the SRS and in many other contaminated environments, an outstanding challenge was that residual drainage from the source zone had never been directly addressed. Lacking this understanding, the dynamics of a plume's trailing edge remains unknown, and

remediation timeframes cannot be predicted. The challenging nature of these problems is reflected in large uncertainties in remediation timeframes at many contaminated sites, even after decades of extensive monitoring and research. Here, we combined data from recently acquired field borehole sediment samples with historical waste disposal records, and long-term groundwater and plume monitoring data. With this, we developed a mixing model to predict source zone recharge rates and contaminant concentrations within the plume as functions of time and distance. The approach developed here is applicable not only at the SRS, but also at other sites with similar long histories of contamination.

EXPERIMENTAL SECTION

Field Borehole Sampling. A map of the Basin-3 area is presented in Figure 1, showing spatial relations among the sampling boreholes, historical monitoring wells, groundwater flow direction, and Fourmile Branch. A total of eight boreholes (0.10 m diameter sediment cores) were drilled; five in August 2008 (FAW-1–5), and three in March 2011 (FAW-6–8). Three of the boreholes (FAW-1, -3, -8, not on the Figure 1 map) were purposely drilled outside of the plume, to obtain "background" samples. FAW-1 is located 300 m west of FAW-2; FAW-8 is located 360 m northwest of FAW-2; and FAW-3 at the down stream of Basin-2. The borehole sediment samples were collected approximately at 1 m intervals, below the nominal water table. The collected samples were immediately sealed in double plastic bags or polypropylene bottles, and refrigerated at 4 °C during transportation and storage. The locations of the three long-term groundwater-monitoring wells FSB-95DR, FSB-110D, and FSB-79 are also indicated on the map (Figure 1, in red).

pH Measurements of Pore Water Samples. The pH was measured by using 1:1 (mass ratio of wet-sediment to deionized-water) diluted pore waters (PWs). These measurements were conducted using the relatively fresh sediment samples (measured onsite, 3 days after sampling) using an Orion 8104BNUWP Ross Ultra rugged bulb pH electrode and pH meter (Thermo Scientific). The pH values were also measured from the directly extracted (described later) PWs. Note that these measurements were conducted at LBNL, 3 months after the sampling. Both sets of data are presented in Supporting Information (SI) Table 1.

Sediment Pore Water Analyses. Pore waters (PWs) were separated from sediment samples of different depths by centrifuge-filtering moisture-preserved sediments (40 g) at 4000 × RCF for 15 min in polypropylene centrifuge tubes with 0.2 µm filter membranes. The collected PWs were measured for their pH and chemical composition. An ion chromatograph (IC, Dionex ICS-2100) was used for analyses of PW anion concentrations. Concentrations of U, other metal ions, and Si were measured using an inductively coupled plasma mass spectrometer (ICP-MS, ELAN DRC II, Perkin-Elmer).

³H Analyses. For each sample, one mL extracted PW was mixed thoroughly with 15 mL scintillation cocktail in a 20 mL scintillation vial, and measured by liquid scintillation analysis (Tri-Carb 2900TR, PerkinElmer). A ³H standard (PerkinElmer) was used to verify the system's performance and efficiency.

Adsorbed U Concentrations in Sediments. Two methods were compared for extracting adsorbed U from the sediment surfaces: NaHCO₃–Na₂CO₃ solution at pH 9.5,¹⁷ and 1% HNO₃ solution. Sediment (4.00 g, moisture-corrected solid mass) was mixed with 40 mL desorption solution and

agitated on a reciprocating shaker for 40 days for the two methods. Two mL aliquots of each suspension were taken and centrifuged at $14000 \times \text{RCF}$ for 30 min. The supernatant solutions were analyzed for U using KPA or ICP-MS. All extractions were done in duplicate. Field partition coefficients (field K_d , mL g^{-1}) were calculated based on these measurements and the U concentrations measured in the PW samples. The term "field K_d " is used to distinguish these values obtained by direct extraction of PWs, from values obtained by laboratory equilibration of batch suspensions.

MODEL DEVELOPMENT

Based on reported local hydrologic parameters,¹⁸ waste composition,⁴ and the geometry of the seepage basin, vadose zone, groundwater, and underlying Tan Clay (Figure 2a.), rates

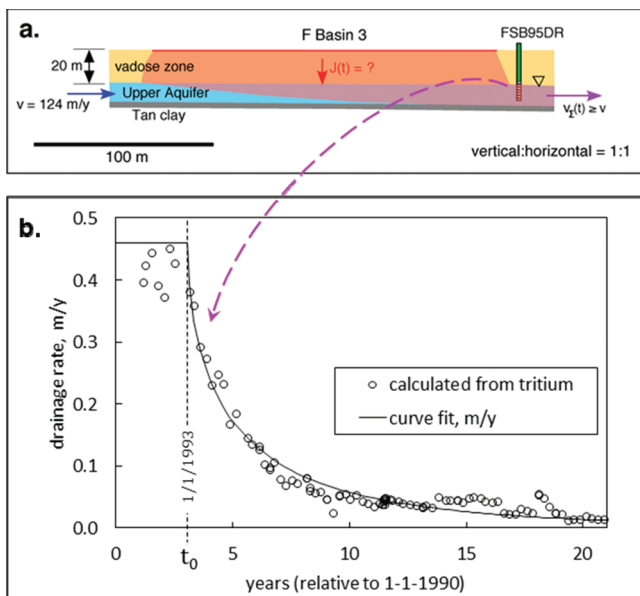


Figure 2. (a.) Conceptual model for vadose zone drainage into the Upper Aquifer; (b.) Model calculated basin drainage rates based on tritium data, and the fitted model curve (eq 1).

of seepage into the Upper Aquifer were recently estimated through calculating fractional contributions of wastewater to groundwaters sampled at well FSB-95DR. These samples consist of a mixture of vadose zone wastewaters and upstream background groundwaters, such that mass balance¹⁶ yields time-dependent drainage fluxes (points plotted in Figure 2b). A smooth functional expression for the seepage rate $J(t)$ (volumetric flow per unit area), is obtained through fitting the drainage fluxes to

$$J(t) = J_0 \exp[-((t - t_0)/\tau)^\beta] \quad (1)$$

where J_0 is the maximum seepage flux of Basin-3 water into the Upper Aquifer, t_0 is the time at which wastewater seepage begins to decrease from J_0 , τ is an empirical decay time, and β is an empirical power term. Based on the recent basin drainage study,¹⁶ J_0 was assigned the value of representative site soil hydraulic conductivity K_s of 0.46 m y^{-1} . Drainage persisted at this rate for about 4.4 years after basin closure. Thus, we set $t_0 = \text{January 1, 1993}$. Setting the adjusting parameters τ and β to 2.02 y and 0.591 , respectively, minimizes the root-mean-square difference (rsmd) between $J(t)$ (eq 1) and the seepage rates

calculated from the tritium data¹⁶ over the full time range shown in Figure 2b to 0.022 m y^{-1} . It should be noted that τ and β are the only adjustable parameters used in the calculations, and they are simply used to provide a continuous functional expression for calculated basin drainage rates. The latter were calculated based solely on parameter values previously reported for the F-Area (no parameter adjustments). Here we extend that approach to predict concentrations of nonreactive contaminants as functions of time and distance away from Basin-3. For this purpose, $J(t)$ was multiplied by the Basin-3 length ($L = 219 \text{ m}$) and the estimated average basin solution ${}^3\text{H}$ and nitrate concentrations to obtain predicted contributions of these contaminants at downstream monitoring wells (per unit traverse sampling width) over time. For ${}^3\text{H}$, radioactive decay (half-life of 12.3 y) was applied to an initial activity of $85\,800 \text{ nCi L}^{-1}$. For nitrate, a basin concentration of 87 mM was assigned.¹⁶ Time dependent contaminant input is diluted by a flux of groundwater upstream of Basin-3, flowing at a Darcy velocity of 31 m y^{-1} (product of the estimated PW velocity v of 124 m y^{-1} times the effective porosity n of 0.25). This background-groundwater flux is weighted by the well screen length ($B = 6.1 \text{ m}$), taken as the vertical water sample integration interval. Thus, immediately downstream of Basin-3 at FSB-95DR, the concentration of ${}^3\text{H}$ or nitrate is estimated as

$$C(t) = \frac{LJ(t)C_0 + BnvC_b}{LJ(t) + Bnv} \approx \frac{LJ(t)C_0}{LJ(t) + Bnv} \quad (2)$$

where C_0 and C_b are its concentration in the basin waters and uncontaminated waters, respectively (decay-corrected in the case of ${}^3\text{H}$). Because $C_0 \gg C_b$ for ${}^3\text{H}$ and nitrate, we will use the approximation on the right-hand side of eq 2.

At distances downstream, $C(t)$ is estimated by incorporating additional dilution from net rainfall infiltration, calculated by multiplying the estimated net infiltration rate I_r at SRS of 0.38 m y^{-1} by the appropriate distance x further downstream from FSB-95DR along the plume path. Thus, for a well along the plume path at distance x , the concentration of a conservative contaminant tracer is given by

$$C(x, t) = \frac{LJ(t - t_x)C_0}{LJ(t - t_x) + Bnv + I_r x} \quad (3)$$

In eq 3, a location-dependent lag time $t_x = x/v$ accounts for travel time from the basin to the monitoring well of interest. Combining eqs 1 and 3 results in

$$\frac{C(x, t)}{C_0} = \frac{\exp\{-[(t - (x/v) - t_0)]^\beta\}}{\exp\{-[(t - (x/v) - t_0)]^\beta\} + \frac{Bnv + xI_r}{LK_s}} \quad (4)$$

The applicability of this dilution model was tested through comparisons with the 20 years of groundwater monitoring data measured at wells FSB-95DR, -110D, and -79 along the plume flow path. The composite uncertainties in $C(x,t)$ are primarily associated with $J(t-t_x)$, and in the range of 0.3–0.5, relative to the calculated $C(x,t)$, not relative to C_0 (SI).

RESULTS AND DISCUSSION

Understanding the Current Plume Through Constructing Chemical Transect Maps. Sampling and analyses to develop three-dimensional plume maps are very expensive when contamination is extensive. Based on previous groundwater sampling, we collected plume sediments and pore waters

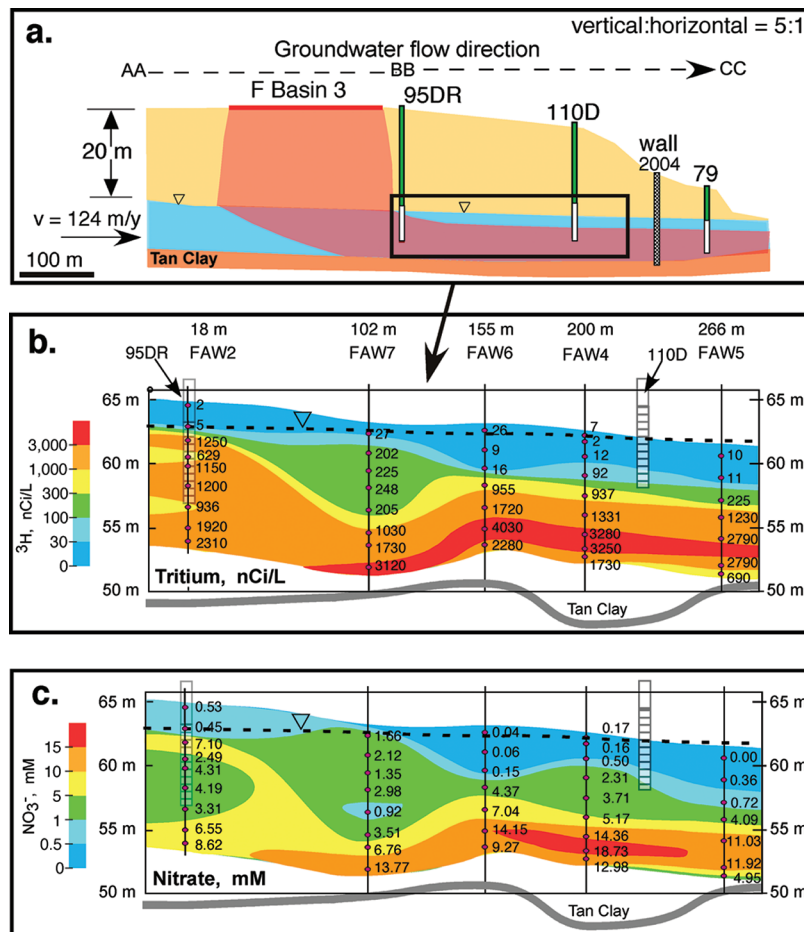


Figure 3. Transect maps of (a.) Basin-3 plume, (b.) ${}^3\text{H}$ aqueous activity, and (c.) nitrate concentrations of the current plume at the F-Area Savannah River Site.

from five new boreholes in order to construct a set of transect maps along the central plume flow line (dashed line BB-CC in Figure 1). The mapped area is within the black frame shown in Figure 3a. The transect crosses borehole FAW-2 (18 m downstream) and is directed toward Fourmile Branch with the boreholes FAW-7, -6, -, and -5 projected on the BB-CC line at the distances 102, 155, 200, and 266 m, respectively. It should be noted that some boreholes are projected onto BB-CC over larger distance than others (Figure 1). Two “non-reactive” elements: NO_3^- and ${}^3\text{H}$ are presented in Figure 3, and two “reactive” elements: H^+ (pH) and U (aqueous U and carbonate-extracted U) are presented in Figure 4. The effectively “non-reactive” behavior of NO_3^- in the F-Area groundwaters is reflected in its close correlation to decay-corrected ${}^3\text{H}$ ¹⁶ and in its isotopic composition,¹⁹ indicative of very low microbial activity. On these transect maps (Figures 3bc and Figure 4), the X-axis corresponds to the distance from the SW-corner of Basin-3 downstream, and the Y-axis is the elevation relative to mean sea level. The elevations of water table (with slope about 0.01) and the low permeability Tan Clay layer as the bottom boundary of the aquifer were drawn with the best available information.⁴ The locations and depths of two historical GW monitoring wells are also shown on these maps. The measured values of ${}^3\text{H}$, NO_3^- , pH, aqueous U, and carbonate-extracted U are presented at sample points along the vertical borehole lines on these transects. The element-by-element discussions are presented next.

Tritium. The initial activity of ${}^3\text{H}$ in the seepage basin waste stream is about 101,609 nCi L⁻¹,⁴ and its half-life 12.3 y. Given its high concentrations in the seepage basin waste stream and its negligible reactivity with sediments and other solutes, ${}^3\text{H}$ serves as an ideal tracer for the migration of the waste plume over time. At the SRS the regional background ${}^3\text{H}$ levels are up to 0.9 nCi/L in the vadose zone and 1.6 nCi L⁻¹ in the groundwater.¹⁶ The EPA’s Maximum Contaminant Level (MCL) for ${}^3\text{H}$ is 20 nCi L⁻¹. Our measured ${}^3\text{H}$ data from directly extracted PWs from all seven boreholes are presented in SI Table 2, and data from the five plume body boreholes were used to construct the cross section map shown as Figure 3b. The transect map shows that the current ${}^3\text{H}$ activity in the plume sediment PWs are up to 4000 nCi L⁻¹, with generally higher activities further downstream of Basin-3, and in the deeper samples. Substantially lower ${}^3\text{H}$ activities were obtained in PWs from the shallower sediments along the plume path, consistent with the net recharge of uncontaminated waters from the vadose zone beyond the seepage basin. High ${}^3\text{H}$ activities (600 to 2300 nCi/L) in all aquifer sediments collected closest to Basin-3 (FAW-2) indicate continued recharge from the basin’s vadose zone. The highest ${}^3\text{H}$ activities are all at the locations around and beyond 100 m downstream of FAW-2, showing that the ${}^3\text{H}$ trailing edge has emerged. The very low ${}^3\text{H}$ activities near the water table and with increasing depth reflect recharge and dilution by rainfall infiltration. The plume is vertically stratified with large differences in ${}^3\text{H}$ activities

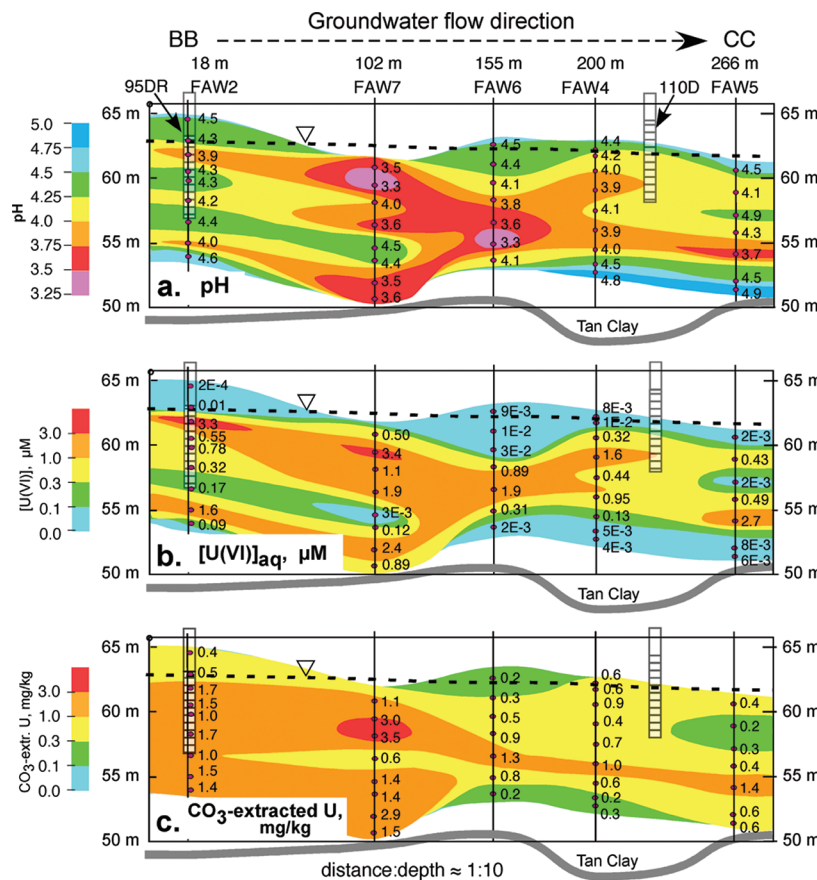


Figure 4. Transect maps of (a.) pH, (b.) U concentrations in pore water, and (c.) adsorbed U (carbonate-extracted from sediments).

between vertically separated samples (~ 1 m gaps), suggesting influences of different reactive facies,²⁰ which are geologically based physiochemical heterogeneities. Although some of the boreholes did not reach the Tan Clay, the pH values of the deepest samples mostly do not suggest that the Tan Clay serves as a significant secondary contaminant source.

Nitrate. The reported average basin waste nitrate concentration is 87 mM.^{4,16} The EPA's MCL for nitrate is 0.71 mM (10 mg L⁻¹ of NO₃⁻-N). The current plume concentration distributions are determined from the sediment PWs. The results of major ion analyses are presented in SI Table 1 (including Na⁺, K⁺, Ca²⁺, Al³⁺, Mg²⁺, Si, NO₃⁻, Cl⁻, F⁻, and SO₄²⁻). Satisfactory charge balance was achieved with an anion:cation charge ratio of 1.039, and r² = 0.997 (SI Figure S1). NO₃⁻ is the major anion (up to 19 mM) in the PWs of the contaminated sediments. Spatial distributions of NO₃⁻ concentrations are very similar to those of ³H. The zone of highest NO₃⁻ concentration (14–19 mM) has migrated downstream to 100 m and beyond, revealing emergence of the NO₃⁻ trailing edge. Note that the NO₃⁻ concentrations are still high (up to 9 mM) at the edge of Basin-3, indicating ongoing slow recharge from the basin's vadose zone. Vertical concentration stratification of NO₃⁻ was similar to that of ³H. Again, lower NO₃⁻ concentrations are measured in the shallower region, due to recharge/dilution by rainfall infiltration. Importantly, the two different nonreactive plume tracers yielded consistent descriptions of plume characteristics.

pH of the Plume. pH is the controlling chemical factor for the behavior of many contaminants. The purpose here is to understand the current plume pH distribution and provide a

basis for predicting its development. As mentioned, systematically higher pH values were obtained from the directly extracted PWs of aged samples, compared to the 1:1 diluted PWs (SI Table 1). Reactions between the PW and sediment apparently caused pH increase during storage. Therefore, the pH values measured from 1:1 diluted fresher samples were used to construct the map shown in Figure 4a. It should be noted that measured pH from 1:1 diluted PWs are higher (by 0.5 unit) than that of groundwater monitoring wells FSB-95DR and FSB-110D (data are not shown). Dilution (DI water) alone cannot explain the extent of the difference. Sediment aging (measured 3 days after the sampling) and exposure to atmosphere might have influenced the results. Although the pH values are probably slightly higher than their corresponding field values, spatial trends and relative values among pH data are expected to be fairly representative of the field plume.

The pH transect map along the flow path through the Upper Aquifer is shown in Figure 4a. The plume pH depends on the source zone recharge, mixing with local groundwater, reactions between PW and sediments, and flow rate. Relative to its former values of about 3, the pH has increased (become more neutral) near the basin, out as far as about 100 m downstream, indicating the development of the trailing plume gradient. Denham and Vangelas³ discussed the importance of determining the dynamics of trailing gradient migration in order to predict times required for attenuating contaminant concentrations. The most acidic pH values were measured primarily at the 100 and 150 m distances, where values less than 3.75 were common. However, a pH of 3.7 was also measured on one sample at 266 m distance. The pH distributions also exhibit

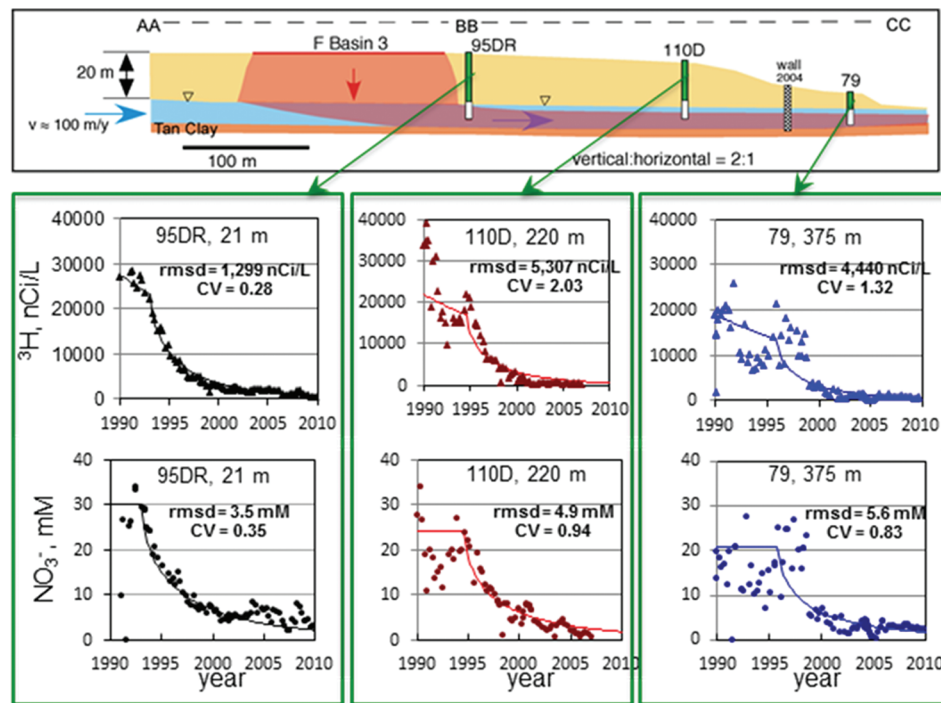


Figure 5. Time-dependent concentrations of ^{3}H and NO_3^- at three different downstream locations. Measurements (points) versus model predictions (curves). Well 79 is located downstream of the base injection line (base-injection started in 2004).

vertical stratification, trending to more neutral values in most of the shallower samples, again reflecting infiltration of uncontaminated soil–water.

Uranium. All the sediment samples were measured for their aqueous and adsorbed U concentrations and the data are presented in SI Table 2. Using these data we constructed two vertical transect maps of aqueous and adsorbed U (Figures 4b,c). The 1% HNO_3 extraction yielded higher U values than those obtained using carbonate, suggesting possible solid phase U dissolution by 1% HNO_3 . Therefore, only the data of carbonate-extracted U were used for the map. It should be noted that because the PWs were extracted from aged sediment (3 months after the sampling day) and the measured pH values are higher than those observed in fresher sediment (1:1 dilution) (SI Table 1), U adsorption likely increased after sampling. The measured pore-water U concentrations are up to $3.4 \mu\text{M}$, about 25 times higher than its MCL. The two U maps exhibit several important features. (a) The zone of highest U concentration has moved away from the source/basin to the same region with the lowest pH, consistent with other indications that the trailing edge of the plume has emerged. (b) The overall U concentrations at the edge of the basin are still high because of the continued slow recharge and migration of U from the basin's vadose zone. (c) The plume is vertically stratified with large differences in U concentration between vertically separated samples. (d) In contrast to the behavior of the nonreactive ^{3}H plume, the shape of the aqueous U plume is similar to that of the pH plume, reflecting pH-dependent U sorption. (e) The aqueous U plume is ahead of the adsorbed U plume, due to slight pH recovery near the source zone. (f) The [U] plume is more dispersed at the down-gradient locations.

The “field” K_d values measured in this work (1.0 to $\sim 10\,000 \text{ L kg}^{-1}$) are correlated with PW pH values (SI Table SI-2 and Figure SI-2) and cations and anion concentrations (SI Table SI-2). These field K_d are in a general agreement with values

determined by Serkiz et al.¹² and by Dong et al.¹³ using laboratory batch U adsorption experiments with SRS F-Area sediments (SI Figure SI-2). The overall K_d values measured in this work are slightly smaller at $\text{pH} < 4.5$ than those of Dong et al. This may possibly have resulted from the higher dissolved cations (Al^{3+} , Ca^{2+} , Mg^{2+}) and anions (e.g., Si, F^-) in the field PW solutions (SI Table SI-2). For example, measured Al^{3+} and Si concentrations in field PWs are as high as 2.0 and 1.5 mM, respectively, whereas Al^{3+} and Si concentrations in the sorption solutions in Dong et al.’s work are much lower. These cations can compete for the sorption sites with U(VI), and the anion can form aqueous complexes with U(VI), which will result in reduced sorption.¹³

Historical Groundwater Monitoring Data. The Basin-3 plume has been extensively monitored from around 1990, one year before the basins were capped.³ We selected three wells having the longest monitoring terms, and examined twenty years of quarterly measurements of nonreactive contaminant ^{3}H and NO_3^- .²¹ Wells FSB-95DR, FSB-110D, and FSB-79, are located at 21, 220, and 375 m down gradient from Basin-3, respectively (Figure 1). The quarterly measured ^{3}H and NO_3^- values from the three monitoring wells are presented in Figures 5.

Comparisons of Model Predictions and Groundwater Data. The assumption that the time trends of ^{3}H and NO_3^- concentrations at the downstream boundary of Basin-3 (in well FSB-95DR) are explained through the time-dependent vadose zone recharge combined with dilution by the background groundwater was shown to be consistent with vadose zone mass balance and best estimates of its representative hydraulic conductivity.¹⁶ Additional dilution from net rainfall infiltration is important at the locations further down gradient from the source (wells FSB-100D and FSB-79). The model described earlier (eqs 1–4) was tested through comparisons with 20 years of ^{3}H and NO_3^- groundwater monitoring data at the three

different locations. In Figure 5 the predicted time trends at these wells are shown as curves in the ${}^3\text{H}$ and nitrate graphs. The rmsd and CV (coefficient of variation) values provide statistical comparisons between each data set and its associated model prediction. Equation 2 was used for FSB-95DR, whereas eq 4 was used for wells FSB-100D and FSB-79. The good match obtained for ${}^3\text{H}$ time trend at FSB-95DR reflects the fact that the basin flux was calibrated to these data. The predicted ${}^3\text{H}$ trend at well FSB-110D captures the general features of the data, although some of the 1990–1991 data exceed the expected activities. Overestimates of ${}^3\text{H}$ activities and NO_3^- concentrations at later times (and highest CVs) likely reflect the fact that well FSB 110D only extends about 3 m into the Upper Aquifer (Figures 3a,b), and samples waters with greater influence from rainfall infiltration. The highly variable ${}^3\text{H}$ activities reported for FSB-79 up to 1998 cannot be fit, but the values at later times are reasonably well matched by the calculations. Variations in rainfall recharge must also contribute to fluctuations in upstream background groundwater flux, which also contribute to dilution variation (SI). The nitrate data are fairly well predicted at the wells FSB-95DR and FSB-110D, whereas the variability in the FSB-79 up to 1998 could not be captured well by the model. In general, relative differences between predictions and data shown in Figure 5 are within about 50%, for concentrations declining by more than an order of magnitude within 20 years, over distances out to 375 m, in a system subject to natural variations in recharge. Thus, the generally good fits to the ${}^3\text{H}$ and nitrate concentration–time data without adjusting parameters support our predictions on the basin's residual drainage as function of time, and effectiveness of groundwater and recharge dilution.

Based on the calculations (eq 1), Basin-3 vadose zone drainage rates currently amount to 2–6% relative to rates during active waste discharge (Figure 2b). However, low residual drainage rates under such near-equilibrium conditions still have significant impact because they introduced 85 800 nCi L^{-1} ${}^3\text{H}$ (decay-adjusted to the initial monitoring date, 2/24/1991), and 87 mM nitrate, while their corresponding MCLs are 20 nCi L^{-1} and 0.7 mM, respectively. It should be noted that current ${}^3\text{H}$ activities at the three monitoring wells remain in the hundreds of nCi L^{-1} , despite appearing to be near-zero in Figure 5. Based on the predicted drainage and dilution rates (and ${}^3\text{H}$ decay rate), reaching the nitrate and ${}^3\text{H}$ MCLs in the Upper Aquifer will take about 10 and 20 more years, respectively. Although there are large uncertainties with these predictions, groundwater contamination long after basin closure persists because (1) waste stream concentrations exceed MCLs by several orders of magnitude, (2) Basin-3 is large (219 m along the groundwater flow path), (3) the contaminated vadose zone is thick (20 m), and (4) later stage vadose zone drainage rates are very slow. At other contaminated sites such as the former seepage basins at the Hanford and Oak Ridge facilities where these factors are present, similarly long recovery times for groundwater quality can be anticipated.

Impacts. Research presented here integrates analyses of new data from field borehole sediments with historical site waste disposal data, regional groundwater data, and plume monitoring data. We developed a mixing model to estimate time-dependent source zone recharge rates and contaminant concentrations within the plume as functions of time and distance. Our plume vertical cross section concentration maps of selected key contaminants revealed for the first time the trailing edges and

concentration gradients of pH and different plume contaminant elements. Our model provides a tool to estimate the current and future time-dependent concentration and distance profiles for the nonreactive species and importantly provides the baseline for the next step on quantitatively understanding the behavior of reactive contaminant elements such as radioisotopes of uranium and iodine. This new information is needed for reliably estimating long-term plume migration and natural attenuation. The approaches presented here are cost-effective means for obtaining critical information for solving practical remediation challenges.

ASSOCIATED CONTENT

S Supporting Information

Text of Uncertainty Analyses for model calculations of flow and concentrations; Table-S1, Major chemical compositions of sediment PWs; Table-S2, Tritium and uranium concentrations for all sediment samples; Figure S1, Charge balance in extracted pore-waters; Figure S2, Comparison of “Field” K_d values of U(VI). This material is available free of charge via the Internet at <http://pubs.acs.org>.

AUTHOR INFORMATION

Corresponding Author

*Phone: 510-486-6004; fax: 510-486-7152; e-mail: jwan@lbl.gov.

Notes

The authors declare no competing financial interest.

ACKNOWLEDGMENTS

The work is supported as part of the Sustainable Systems (SS) Scientific Focus Area (SFA) program at LBNL, supported by the U.S. Department of Energy, Office of Science, Office of Biological and Environmental Research, Subsurface Biogeochemical Research Program, through Contract No. DE-AC02-05CH11231 between LBNL and the U.S. DOE. Field samples and support for Miles Denham were provided by the Applied Field Research Initiative at SRNL funded by the U.S. Department of Energy Office of Environmental Management. We thank the associate editor Dr. Dzombak and the three anonymous reviewers for their constructive comments and suggestions.

REFERENCES

- (1) SRNS. *Annual Corrective Action Report for the F-area Hazardous Waste Management Facility, the H-area Hazardous Waste Management Facility, and the Mixed Waste Management Facility*; Savannah River Nuclear Solutions: Aiken, SC, 2010.
- (2) Looney, B. B.; Grant, M. W.; King, C. M. *Estimation of Geochemical Parameters for Assessing Subsurface Transport at the Savannah River Site*, DPST-85-904; E.I. Du Pont de Nemours & Co.: Wilmington, DE, 1987.
- (3) Denham, M.; Vangelas, K. M., Biogeochemical gradients as a framework for understanding waste-site evolution. *Remediation* 2008, Winter 2008, 5–17.
- (4) Killian, T. H.; Kolb, N. L.; Corbo, P.; Marine, I. W. *Environmental Information Document F-Area Seepage Basins*; E. I. du Pont de Nemours & Co. Savannah River Laboratory: 1987; p 203.
- (5) Jean, G. A.; Yarus, J. M.; Flach, G. P.; Millings, M. R.; Harris, M. K.; Chambers, R. L.; Syms, F. H. Three-dimensional geologic model of southeastern Tertiary coastal-plain sediments, Savannah River site, South Carolina: An applied geostatistical approach for environmental applications. *Environ. Geosci.* 2004, 11 (4), 205–220.

- (6) Seaman, J. C.; Bertsch, P. M.; Strom, R. N. Characterization of colloids mobilized from southeastern coastal plain sediments. *Environ. Sci. Technol.* **1997**, *31* (10), 2782–2790.
- (7) Zhang, S.; Du, J.; Xu, C.; Schwehr, K. A.; Ho, Y. F.; Li, H. P.; Roberts, K. A.; Kaplan, D. I.; Brinkmeyer, R.; Yeager, C. M.; Chang, H. S.; Santschi, P. H. Concentration-dependent mobility, retardation, and speciation of iodine in surface sediment from the Savannah River site. *Environ. Sci. Technol.* **2011**, *45* (13), 5543–5549.
- (8) Seaman, J. C.; Looney, B. B.; Harris, M. K. Research in support of remediation activities at the Savannah River site. *Vadose Zone J.* **2007**, *6* (2), 316–326.
- (9) Kaplan, D. I.; Bertsch, P. M.; Adriano, D. C. Enhanced transport of contaminant metals through an acidic aquifer. *Ground Water* **1995**, *33*, 708–717.
- (10) Dai, M.; Kelley, J. M.; Buesseler, K. O. Sources and migration of plutonium in groundwater at the Savannah River site. *Environ. Sci. Technol.* **2002**, *36*, 3690–3699.
- (11) Wan, J. M.; Dong, W. M.; Tokunaga, T. K. Method to attenuate U(VI) mobility in acidic waste plumes using humic acids. *Environ. Sci. Technol.* **2011**, *45* (6), 2331–2337.
- (12) Serkiz, S. M.; Johnson, W. H.; Wile, L. M. J.; Clark, S. B. Environmental availability of uranium in an acidic plume at the Savannah River site. *Vadose Zone J.* **2007**, *6* (2), 354–362.
- (13) Dong, W.; Tokunaga, T. K.; Davis, J. A.; Wan, J. Uranium(VI) adsorption and surface complexation modeling onto background sediments from the F-Area Savannah River site. *Environ. Sci. Technol.* **2012**, *46*, 1565–1571.
- (14) Otosaka, S.; Schwehr, K. A.; Kaplan, D. I.; Roberts, K. A.; Zhang, S.; Xu, C.; Li, H. P.; Ho, Y. F.; Brinkmeyer, R.; Yeager, C. M.; Santschi, P. H. Factors controlling mobility of ^{127}I and ^{129}I species in an acidic groundwater plume at the Savannah River site. *Sci. Total Environ.* **2011**, *409* (19), 3857–65.
- (15) Kaplan, D. I.; Roberts, K. A.; Schwehr, K. A.; Lilley, M. S.; Brinkmeyer, R.; Denham, M. E.; Diprete, D.; Li, H. P.; Powell, B. A.; Xu, C.; Yeager, C. M.; Zhang, S. J.; Santschi, P. H. Evaluation of a radioiodine plume increasing in concentration at the Savannah River site. *Environ. Sci. Technol.* **2011**, *45* (2), 489–495.
- (16) Tokunaga, T. K.; Wan, J.; Denham, M. E. Estimates of vadose zone drainage from a capped seepage basin, F Area, Savannah River site. *Vadose Zone J.* **2012**, in press.
- (17) Kohler, M.; Curtis, G. P.; Meece, D. E.; Davis, J. A. Methods for estimating adsorbed uranium(VI) and distribution coefficients of contaminated sediments. *Environ. Sci. Technol.* **2004**, *38* (1), 240–247.
- (18) Chase, J. *F-Area Hazardous Waste Management Facility Corrective Action Report* (U); Westinghouse Savannah River Company: Aiken, SC, 1999; p 413.
- (19) Christensen, J. N.; Conrad, M. E.; Bill, M.; Denham, M.; Wan, J.; Rakshit, S.; Stringfellow, W. T.; Spycher, N. Isotopic systematics (U, nitrate, and Sr) of the F-Area acidic contamination plume at the Savannah River site: Clues to contaminant history and mobility. In *American Geophysical Union Fall Meeting*; American Geophysical Union: San Francisco, 2010; Vol. H23D-1229.
- (20) Sassen, D. S.; Hubbard, S. S.; Spycher, N.; Chen, J.; Denham, M. E., Utilizing geophysics to spatially distribute reactive transport parameters using a reactive facies concept. in review.
- (21) Denham, M. E. *Groundwater Data for Monitoring Wells FSB-9SDR and FSB-110D*; Savannah River National Laboratory: Aiken, SC, 2011.